13th World Conference on Earthquake Engineering
Vancouver, B.C., Canada
August 1-6, 2004
Paper No. 3282

ELASTO-PLASTIC RESPONSE ANALYSIS OF A COMPLICATED SHIELD TUNNEL SYSTEM SUBJECTED TO INCIDENT SEISMIC WAVES

Tong JIANG[1] , Liang SU[2]

SUMMARY

According to the analysis model of the equivalent continuity stiffness of the shield lining, this paper builds up a practical procedure to evaluate the elasto-plastic stress developed in a complicated shield tunnel system subjected to incident seismic waves. The shield lining is simulated by the beam supported on soil, having the same stress-deformation relation as that of the original segments-joint structure. The finite element method has been used to calculate the internal forces when a seismic wave passing the shield tunnel. The calculated results show that the transition stress caused by wave propagation could reach a significant value in comparison with the case of stable harmonic wave. As a numerical example, the procedure is applied to analyze the stresses of Yanan East Road Tunnels across the Huangpu River in Shanghai subjected to several practical seismic waves. The numerical results displayed that the stresses near the joint of the shield tunnel and the vertical vent shaft are rather lager than that generated in general region of the tunnel. The numerical results also show that the transient stress, the stress concentration and the frequency characteristics of the seismic waves are the important factors to influence the seismic stress distribution in the shield tunnel.

INTRODUCTION

The authors have developed a practical method to evaluate the longitudinal stiffness of shield tunnel. The segment and joint of the shield tunnel are simulated as the equivalent uniform beam, having the same stress-deformation relation as that of the original shield lining system. The elasto-plastic behaviors of the straight shield tunnel with uniform lining section and homogeneous soil condition under the actions of

seismic wave propagation and earthquake-induced settlement have been analyzed. The fundamental characteristics of seismic stress developed in tunnel are investigated by parametric studies. As a numerical example, the seismic stresses in the longitudinal direction of Shanghai Yanan East Road tunnel across the Huangpu River have been calculated [1][2][3].

But a practical tunnel system usually is a complicated structure system. The structures of the vertical vent shaft, the continuous tunnel in the lead line and the main shield tunnel are different. At the meantime, the tunnel section, joint are not uniform and soil condition is not homogeneous. Fig.1 [4] showed the schematic diagram of Shanghai Yanan East Road tunnel across the Huangpu River. It consists of the lead line made of continuous tunnel (with rectangle section), the vertical vent shaft No.1~No.3 (with rectangle or circle section), and the main shield tunnel. In order to analyze the seismic stress of the complicated tunnel system, the above-mentioned simple model is not appropriate. This paper analyzes further the seismic stress developed in the complicated tunnel system under the action of seismic wave propagation by using the FEM.

In the analytical model the following assumptions have been made: let the soil and the lining retain elasticity but consider the elasto-plasticity of the joints in the longitudinal direction of the tunnel. The shield tunnel has been simulated as an elasto-plastic beam supported on elastic soil with the stiffness equivalent to that of segments-joint system. The main shield tunnel, the vertical vent shaft and the continuous tunnel in the lead line have been divided into finite elements respectively. The seismic stress of the tunnel system subjected to obliquely incident P or SV seismic waves has been analyzed.

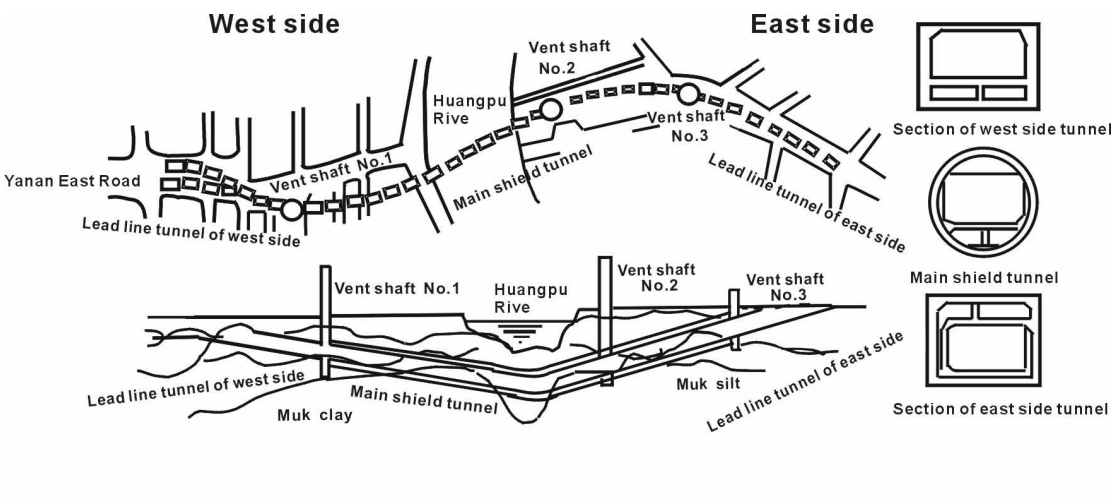

Fig.1 System of Shanghai Yanan East Road tunnel across the Huangpu River

OUTLINE OF THE FEM

FEM Discretization of the Tunnel System

The main shield tunnel, the vertical vent shaft and the continuous tunnel in the lead line have been divided

into beam finite elements respectively. For a beam element having length of L the element stiffness matrices $[K]^e_{pipe}$ is showed in Eq.(1)

$$[K]^e_{pipe} = \begin{bmatrix} \frac{EA}{L} & 0 & 0 & -\frac{EA}{L} & 0 & 0 \\ & \frac{12EI}{L^3} & \frac{6EI}{L^2} & 0 & -\frac{12EI}{L^3} & \frac{6EI}{L^2} \\ & & \frac{4EI}{L} & 0 & -\frac{6EI}{L^2} & \frac{2EI}{L} \\ & & & \frac{EA}{L} & 0 & 0 \\ & symmetry & & & \frac{12EI}{L^3} & -\frac{6EI}{L^2} \\ & & & & & \frac{4EI}{L} \end{bmatrix} \tag{1}$$

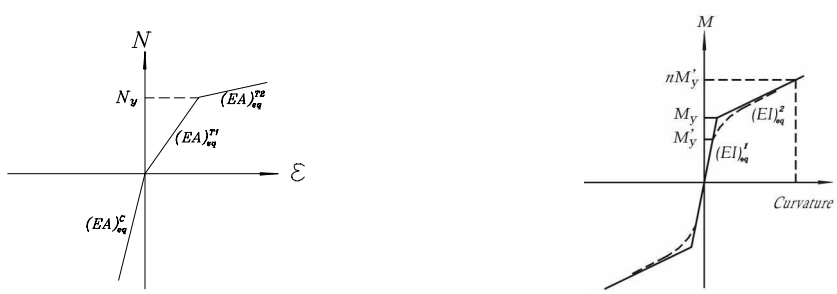

(a) Axial Stiffness (b) Bending stiffness

Fig.2 Equivalent stiffness of shield tunnel

The assumption, that the vertical vent shaft and the continuous tunnel in the lead line retain elasticity, has been made. The equivalent stiffness of the shield tunnel elements can be obtained as follows:

Equivalent axial stiffness (Fig.2.a)

$$EA = \begin{cases} (EA)^C_{eq} & (N \le 0) \\ (EA)^{T1}_{eq} & (0 < N < N_y) \\ (EA)^{T2}_{eq} & (N_y \le N) \end{cases} \tag{2}$$

Equivalent bending stiffness (Fig.2.b)

$$EI = \begin{cases} (EI)^1_{eq} & (|M| < M_y) \\ (EI)^2_{eq} & (M_y \le |M|) \end{cases} \tag{3}$$

where: $(EA)^C_{eq}$ = Equivalent compression stiffness

$(EA)^{T1}_{eq}, (EA)^{T2}_{eq}$ = Elastic and elasto-plastic equivalent tension stiffness

$(EI)^1_{eq}, (EI)^2_{eq}$ = Elastic and elasto-plastic equivalent bending stiffness

N_y, M_y = Equivalent elastic limit axial force and bending moment of the shield tunnel respectively

The calculation formulations of the stiffness in Eq.(2) and Eq.(3) can be found in reference [1].

For a soil element having length of L the element stiffness matrices $[K]^e_{soil}$ is showed in Eq.(4)

$$[K]^e_{Soil} = \begin{bmatrix} \frac{K_a L}{3} & 0 & 0 & \frac{K_a L}{6} & 0 & 0 \\ & \frac{13K_b L}{35} & \frac{11K_b L^2}{210} & 0 & \frac{9K_b L}{70} & -\frac{13K_b L^2}{420} \\ & & \frac{K_b L^3}{105} & 0 & \frac{13K_b L^2}{420} & -\frac{K_b L^3}{140} \\ & & & \frac{K_a L}{3} & 0 & 0 \\ & symmetry & & & \frac{13K_b L}{35} & -\frac{11K_b L^2}{210} \\ & & & & & \frac{K_b L^3}{105} \end{bmatrix} \tag{4}$$

where: K_a, K_b = Axial and lateral spring coefficients of soil

By using the stiffness matrix of beams $[K]_{pipe}$ and the stiffness matrix of soil $[K]_{soil}$, the total stiffness matrix of tunnel system $[K]$ can be obtained as

$$[K] = [K]_{pipe} + [K]_{soil} \tag{5}$$

Omitting the inertia action and using pseudo-dynamic method, the equilibrium equation of the total tunnel system under action of the seismic ground deformation $\{U_g\}$ can be written as

$$([K]_{pipe} + [K]_{soil}) \cdot \{U\} = [K]_{soil} \cdot \{U_g\} \tag{6}$$

Elasto-plastic Analysis of Total Tunnel System

By using the FEM, the difference between the compression and the tension stiffness, and the difference between the elastic bending and plastic bending stiffness for every shield tunnel element has to be considered. According to the axial force and the bending moment of every shield tunnel element, the element stiffness is determined. For every calculating step, the element stiffness is assumed the same as that of last step. After checking the axial force and the bending moment of every shield tunnel element, the element stiffness is modified until the stiffness agrees with the internal forces.

When the seismic wave passes the tunnel system, the distribution of the seismic deformation along the tunnel is different. So the stress analysis under action of seismic deformation can be considered as a procedure of stress analysis under action of deformation for every time interval. Assuming every time interval as one deformation step and during the step the stiffness fixed, the expression in Eq.(4) can be rewritten increment linear relation as Eq. (7),

$$([K]_{pipe} + [K]_{soil}) \cdot \{\Delta U\} = [K]_{soil} \cdot \{\Delta U_g\} = \{R\} \tag{7}$$

where: the stiffness matrix of shield tunnel $[K]_{pipe}$ depends on the internal forces situation of the structure

Accumulating the displacement increment and the internal forces increment for every step, the present displacement and internal forces developed in every element can be obtained. Then the compression and the tension stiffness, and the elastic or plastic bending stiffness for every shield tunnel element can be determined. After assembling a new stiffness matrix, a new step begins until the seismic wave passes the whole tunnel system.

Analysis Procedure under Action of Wave Propagation

Fig.3 shows plane wave propagation with incidence angle θ, velocity C and duration T under Cartesian coordinate. Using the figure the seismic deformation for every tunnel node can be derived.

Assuming the wave front reach point $A\ (x_0, y_0)$ at time t, the delay time of wave front propagating from point A to point $B\ (x_B, y_B)$ t_{AB} can be calculated as

$$t_{AB} = \frac{\cos\theta(x_B - x_0) + \sin\theta(y_B - y_0)}{C} \tag{8}$$

Refer to one-dimensional wave [5], the seismic ground deformation of B point at time t can be obtained

$$U_{gB} = \begin{cases} 0 & t - t_{AB} < 0 \\ \Delta_{\max} f(t - t_{AB}) & T \geq t - t_{AB} \geq 0 \\ 0 & t - t_{AB} \geq T \end{cases} \tag{9}$$

where: f is the; $\Delta_{\max}$ is the normalized seismic displacement time history

$\Delta_{\max}$ is the maximum displacement

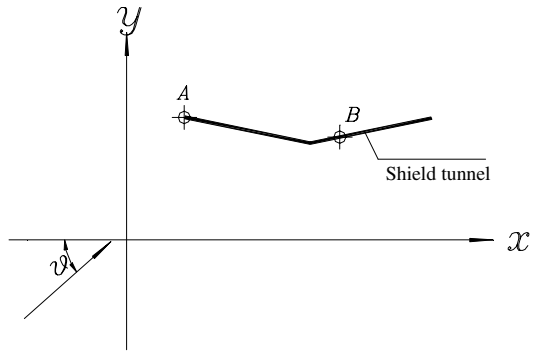

Fig.3 The displacement calculation subjected to plane waves

Assuming the time interval of the seismic displacement time history is Δt and the time interval number is N for duration T, for $t = n\Delta t$ Eq.(9) can be rewritten as

$$U_{gB} = \begin{cases} 0 & n - m < 0 \\ \Delta_{\max}[f_{n-m} + \dfrac{(f_{n-m} - f_{n-m+1})(\alpha_B - m)}{\Delta t}] & N \geq n - m \geq 0 \\ 0 & n - m \geq N \end{cases} \tag{10}$$

where: $\alpha_B = \dfrac{t_{AB}}{\Delta t}$; m is the integral number of x_B

For seismic plane P wave, the component in x axis of U_{gB} is $U_{gB}\cos\theta$ and the component in y axis of U_{gB} is $U_{gB}\sin\theta$; for seismic plane SV wave, the component in x axis of U_{gB} is $-U_{gB}\sin\theta$ and the component in y axis of U_{gB} is $U_{gB}\cos\theta$.

As a whole, the step of calculating the elasto-plastic seismic stress developed in shield tunnel under action of wave propagation can be summarized as follows:

(1) Form stiffness matrixes of total tunnels and soil, and assemble total stiffness matrix.

(2) Calculate ground displacement increment $\{\Delta U_g\}_i$ at time step i and compute the value

$$\{R\}_i = [K]_{soil} \cdot \{\Delta U_g\}_i$$

(3) Apply $\{R\}_i$ on the tunnel system and calculate the elasto-plastic stress based on the method mentioned in above section

(4) According the axial force and the bending moment of every shield tunnel element, modify the element stiffness
(5) Repeat the from step (2) to step (4) until the seismic wave passed the whole tunnel system

NUMERICAL EXAMPLES AND CALCULATING RESULTS

Verification of the applicability and the reliability of FEM

In order to verify the reliability of FEM for analyzing the elasto-plastic stress developed in shield tunnel, comparison between the results of FEM and the analytical method [1] has been made.

The analysis object is the straight shield tunnel with uniform lining section and homogeneous soil condition. The size and the material parameters are: external diameter $D_e = 11m$ and internal diameter $D_i = 9.5m$; Young's modulus of segment is $E_c = 3.45\times10^4 N/mm^2$ and that of joint bolts $E_s = 2.06\times10^5 N/mm^2$; boil's number is $n = 32$, diameter $d = 36mm$, length $l = 0.4m$, yield stress $\sigma_y = 170N/mm^2$; length of segment is $1m$. The stiffness coefficient of soil is $k_0 = 8N/cm^2$ ($K_a = K_b = k_0 D_e$). The waveform is taken as three sine-shaped time history with period $T = 3.5\sec$. The element length is 2 m and the wave velocity of soil is 200 m/s, so the wavelength is 500 m. Based on the earthquake hazard analysis of Shanghai area [6], the amplitudes of seismic ground displacement according to three levels of the earthquake intensity described by exceeding probability for 50 years (63.5%, 10% and 3%) are 1, 5 and 23 cm.

Fig. 4 and Fig. 5 show the moment and axial force time histories under action of sine ground displacement with amplitude 5 cm for incidence angles 0° and 45° respectively. In the figures the part AB shows the internal forces when the second sine wave passes the element, the values of the internal forces are agree with that obtained by analytical method. Table 1 and table 2 shows the maximum internal forces of three earthquake levels obtained by FEM and analytical method respectively. The values obtained by two methods are very close each other.

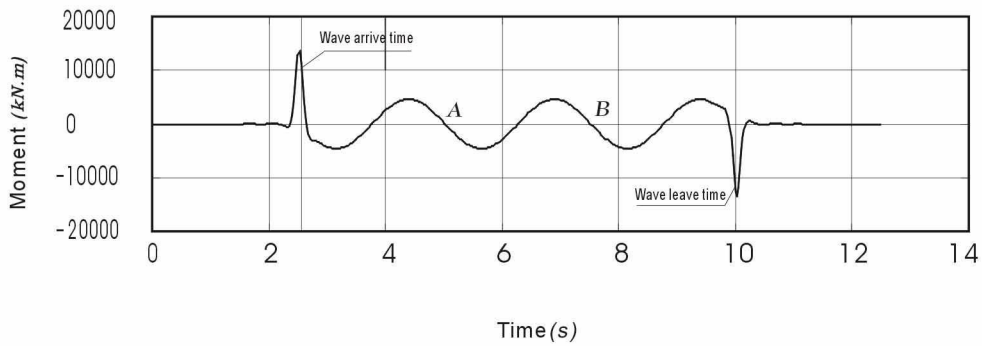

Fig.4 Moment time history developed in shield tunnel for sine wave,(incidence angle=0°

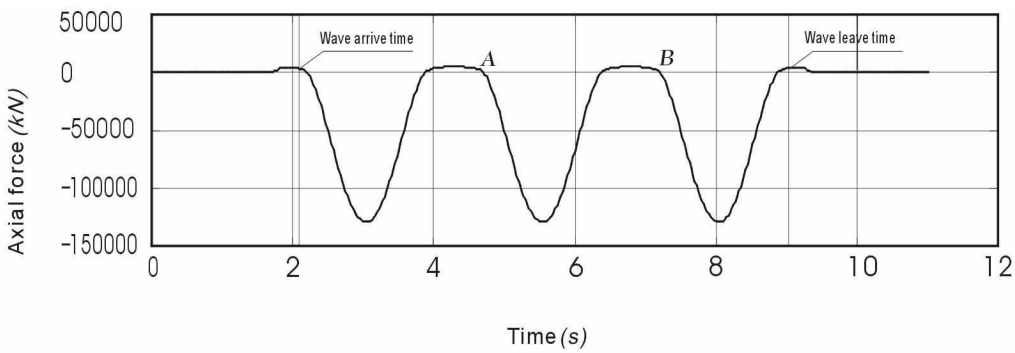

Fig.5 Axial force time history developed in shield tunnel for sine wave, incidence angle=45°

From the figures, the internal forces developed in shield tunnel reach bigger values at the moment when the wave arrived or leaved the element. Especially for Fig. 4 the instantaneous value of the moment exceeded the maximum value calculated by analytical method greatly. We can call the state that occurs before or after the time of wave arriving the element as transient phenomenon. The transient phenomenon is caused by that the distribution of ground displacement deflects one side of the tunnel when the wave arrived or leaved the element. In order to understand the fact of the transient phenomenon, Table 3 shows the effect of different wave velocities (wavelengths) on the maximum moment under action of sine ground displacement with amplitude 5 cm for incidence angles 0°. From Table 3, the larger the wave velocity (wavelength) is, the larger the ratio between the maximum moment and the moment at part AB larger is.

According to the above-mentioned calculated results, we can summarize as follows: (1) Under action of sine-shaped displacement wave the results of internal forces developed in shield tunnel obtained by analytical method and FEM are very close, the applicability and the reliability of FEM have been verified. (2) When the wave passes the tunnel element the transient phenomenon of internal force occurs, the larger the wave velocity (wavelength) is, the more remarkable the transient phenomenon becomes.

Table 1 Results of maximum moment developed in shield tunnel subjected to sine wave with incidence angle 0°for two methods

Amplitude of ground	$M_{\max}(kN \cdot m)$		$M_{\max} > M_y$	Errors (%)
	Analytical	Part AB of FEM		
1.0	914	914	No	0
5.0	4573	4573	No	0
23.0	21038	21032	No	0.03

Table 2 Results of maximum internal force developed in shield tunnel subjected to sine wave with incidence angle 45°for two methods

Amplitude of ground	$N_{\max}(kN)$		$N_{\max} > N_y$	Errors (%)
	Analytical	Part AB of FEM		
1.0	914	914	No	0
5.0	4573	4573	No	0.04
23.0	21038	21032	Yes	3.16

Table 3 Effect of wave velocity on maximum moment developed in shield tunnel

Wave velocity (m/s)	Transient phenomenon		Part AB		Ratio
	$M_{\max}(kN \cdot m)$	$M_{\max} \geq M_y$	$M_{\max}(kN \cdot m)$	$M_{\max} \geq M_y$	
50.0	29902	Yes	29354	Yes	1.02
100.0	26133	No	18235	No	1.43
200.0	13608	No	4573	No	2.98
500.0	5516	No	735	No	7.5
800.0	3453	No	293	No	11.8

Numerical Example of Complicated Shield Tunnel under Action of Practical Seismic Waves

Fig.6 is the calculating schematic diagram of Shanghai Yanan East Road tunnel across the Huangpu River. The practical 3-dimensional tunnel system showed in Fig.1 has been simplified to 2-dimensional calculating plane. The angles θ_1 and θ_2 are the gradient of the tunnels, equal to 3°. The system consists of the lead line made of continuous concrete tunnel with rectangle section $b \times h$ =12.0 $m \times$ 8.0 m and thickness 0.65 m, the vertical vent shaft No.1 with circle section $D = 28.6\,m$ and thickness

0.7 m, the vertical vent shaft No.2 and No.3 with rectangle section 24.3 $m \times 28.2\ m$ and 20.7 $m \times 17.0\ m$, and thickness 1.3 m and 1.0 m respectively. The size and material parameter of the mail shield tunnel and ground soil is the same as above-mentioned. The calculation results verified the assumption of the vertical vent shaft and the continuous tunnel in the lead line retaining elasticity is correct.

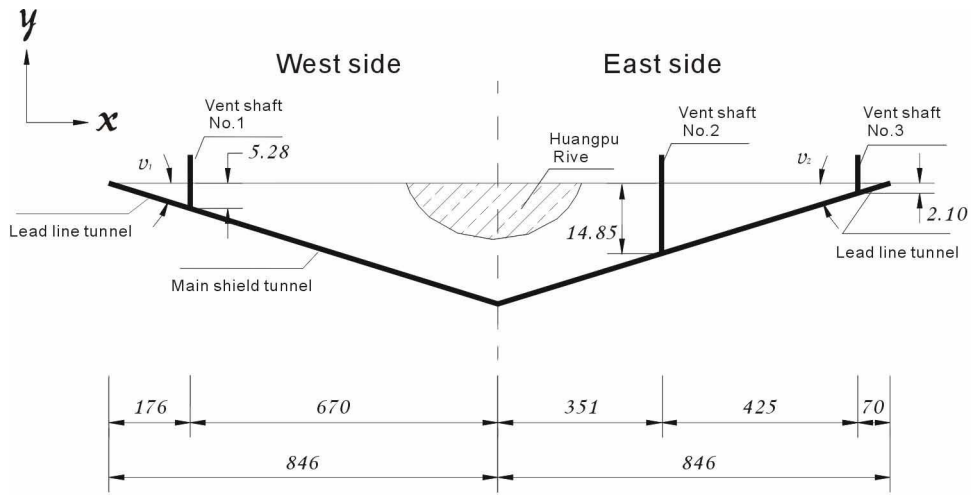

Fig.6 Calculating plane of Shanghai Yanan East Road tunnel across the Huangpu River (Unit: m)

During the numerical analysis, three seismic ground motion records are selected. They are EL Centro wave (1940, USA), Tianjin wave (1976, CHN) and Hyogo-ken Nanbu wave (1995, JPN). The normalized displacement time history of Hyogo-ken Nanbu seismic wave is showed in Fig.7. The wave velocity is assumed as 500 m/s with maximum amplitude 5 cm and incidence angle 0° and 45°. The response of moment and axial force developed in the tunnel system has been calculated by using the method mentioned in the above section. One example of the maximum moment and axial force time history developed in shield tunnel element under action of Hyogo-ken Nanbu seismic wave has been showed in Fig.8 and Fig.9.

The calculating results showed that the maximum internal forces always occurred in the elements located near the joint places of tunnel and vertical vent shaft. In order to compare with other normal tunnel element, Table 4 shows the ratios of moment and axial tension force developed in the joint element and normal element respectively under action of three seismic waves with wave velocity 500 m/s and maximum amplitude 5 cm.

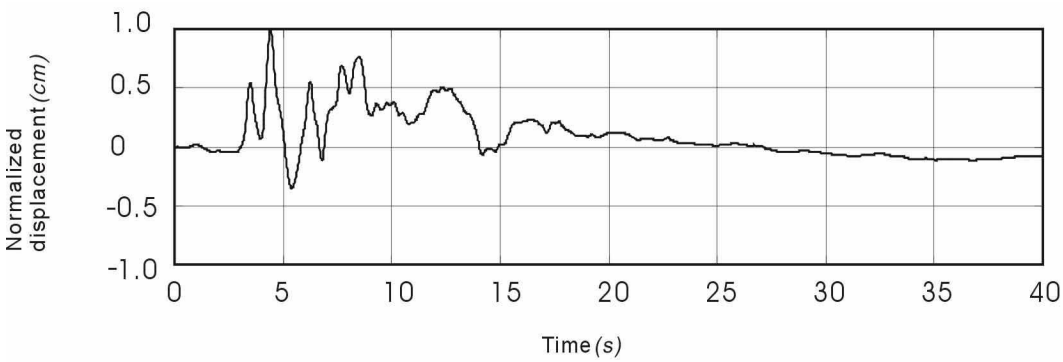

Fig.7 Displacement time history of Hyogo-ken Nanbu seismic wave (1995,JPN)

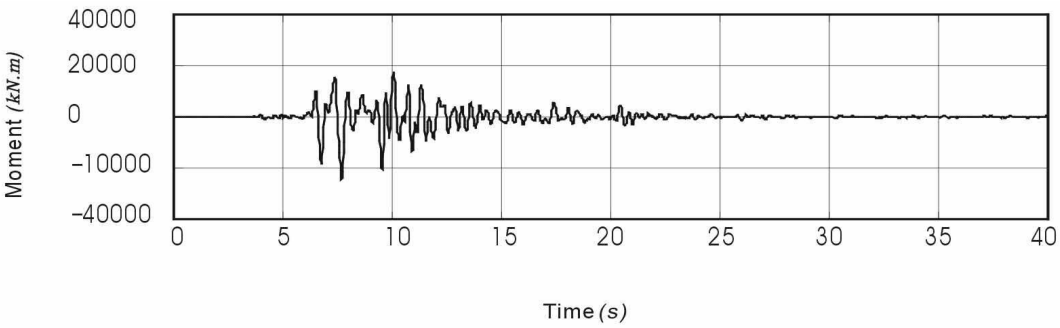

Fig.8 Moment time history developed in maximum internal element
(Hyogo-ken Nanbu seismic wave, $v = 500\, m/s$, incidence angle=0°)

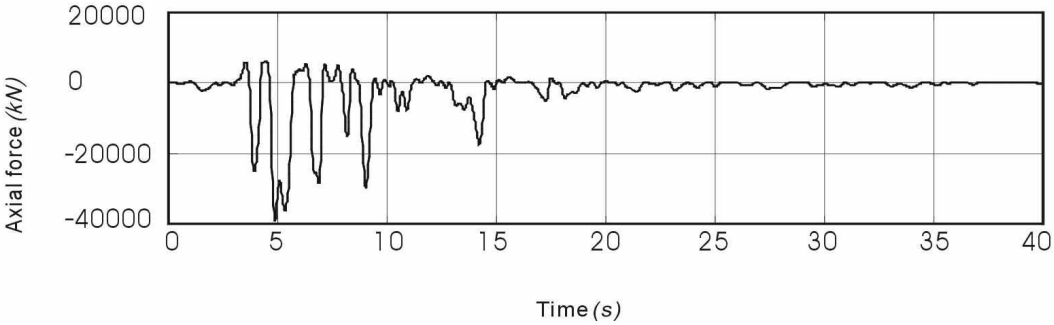

Fig.9 Axial force time history developed in maximum internal element
(Hyogo-ken Nanbu seismic wave, $v = 500\, m/s$, incidence angle=45°)

From the table, the ratios of the joint element and normal element are: for moment are 1.13～2.89 and for axial tension force are 1.18～2.03. The results display that due to the stress concentration occurred near the joint places of tunnel and vertical vent shaft, the ratios of the internal forces developed in the joint element and normal element can reach 1～3. In addition, the effect of different seismic wave on stress concentration is different. By analyzing the Fourier components of three seismic waves, the order of higher frequency component or long wavelength is EL Centro wave, Tianjin wave and Hyogo-ken Nanbu wave. So the wave including the high frequency component can induce larger internal forces in normal

elements as shown in Table 4. Conversely, however, the effect of stress concentration is opposite tendency, namely the order of larger internal forces developed in joint elements showed in Table 4 is Hyogo-ken Nanbu wave, Tianjin wave and EL Centro wave. Thereby several different seismic waves should be chosen for analyzing the seismic response of complicated tunnel system.

The calculating results also showed that the maximum moment and the tension force developed in shield tunnel can exceed the elastic limit moment or elastic limit tension under action of practical seismic waves with wave velocity 500 m/s and maximum amplitude 5 cm. The shield tunnel will work in elaso-plastic situation under action of the earthquake intensity with exceeding probability 10% for 50 years.

Table 4(a) Ratio of moment in joint and normal elements (incidence angle 0°)

Seismic wave	Joint element		Normal element		Ratio
	$M_{\max}(kN \cdot m)$	$M_{\max} > M_y$	$M_{\max}(kN \cdot m)$	$M_{\max} > M_y$	
El-centro	32371	Yes	28634	Yes	1.13
Tianjin	29767	Yes	15837	No	1.88
Hyogo-ken Nanbu	12193	No	4220	No	2.89

Table 4(b) Ratio of axial force in joint and normal elements (incidence angle 45°)

Seismic wave	Joint element		Normal element		Ratio
	$N_{\max}(kN)$	$N_{\max} > N_y$	$N_{\max}(kN)$	$N_{\max} > N_y$	
El-centro	6588	Yes	5605	Yes	1.18
Tianjin	5879	Yes	4899	No	1.20
Hyogo-ken Nanbu	5762	Yes	2838	No	2.03

CONCLUSIONS

Based on the model of the equivalent uniform beam that holds the same stress-deformation relation as that of the original shield tunnel of segment-joint system, this paper analyzes the seismic stress developed in the complicated tunnel system under the action of seismic wave propagation by using the FEM.

In order to verify the reliability of FEM for analyzing the elasto-plastic stress developed in shield tunnel, comparison between the results of FEM and the analytical method had been made. Under the action of sine-shaped displacement wave the results of internal forces developed in shield tunnel obtained by the analytical method and FEM are very close, and the reliability of FEM have been verified.

When the wave passes the tunnel element the transient phenomenon of internal force occurs, the larger the wave velocity (wavelength) is, the more remarkable the transient phenomenon becomes. The transient phenomenon should be noted in the seismic design of shield tunnels.

By using the FEM, the seismic responses of Shanghai Yanan East Road tunnel under action of three practical seismic waves have been analyzed. The tunnel is across the Huangpu River and consists of the vertical vent shaft, the continuous tunnel in the lead line and the main shield tunnel.

The numerical results showed that the existence of the vertical vent shaft could exert influence upon the seismic stress developed in shield tunnel. The maximum internal forces always occurred in the elements located near the joint places of tunnel and vertical vent shaft. The effect of different seismic wave on stress concentration was different. Thereby several different seismic waves should be chosen for analyzing the seismic response of complicated tunnel system.

REFEFENCES

1. Jiang T, Su L. " Elasto-plastic stress analysis of shield tunnels under earthquake action." Chinese Journal of Geotechnical Engineering; 21 (2): 200-204.
2. Jiang T, Su L. "Elasto-plastic stress analysis in the longitudinal direction of shield tunnels during earthquakes." Proceedings of Third China-Japan-US Trilateral Symposium on Lifeline Earthquake Engineering, Kunming, China: 149-156,1988.
3. Jiang T, Su L. "Elasto-plastic stress analysis of shield tunnels under earthquake induced settlement." Proceedings of 5th National Conference on Earthquake Engineering, Beijing, China: 685-690,1998
4. Proceedings on Construction Technique of Yanan East Road tunnel, Shanghai: Shanghai Science and Technology Press, 1992.
5. Wang L.R.L. "Static and quasi-static seismic analysis of buried pipelines." Technical Report No.11, Department of Civil Engineering and Structural Dynamics, Rensselaer Polytechnic Institute, 1980.
6. Research Report on Seismic Microzonation of Shanghai City, Shanghai: Tongji University, 1992.

---

[1] Professor, Research Institute for Structural Engineering and Disaster Reduction, Tongji University, Shanghai, China. Email: jt@mail.tongji.edu.cn

[2] Engineer, Zhejiang Chengjian Design Institute, Hangzhou, Zhejiang, China. Email: sul@hzcnc.com